## STABILITY AND ERROR ANALYSIS FOR A SECOND-ORDER FAST APPROXIMATION OF THE LOCAL AND NONLOCAL DIFFUSION EQUATIONS ON THE REAL LINE\*

CHUNXIONG ZHENG $^{\dagger}$ , QIANG DU $^{\ddagger}$ , XIANG MA $^{\S}$ , AND JIWEI ZHANG $^{\P}$ 

**Abstract.** The stability and error analysis of a second-order fast approximation are considered for the one-dimensional local and nonlocal diffusion equations in the unbounded spatial domain. We first use the conventional central difference scheme to discretize the local second-order spatial derivative operator and use an asymptotically compatible difference scheme to discretize the spatial nonlocal diffusion operator, and apply second-order backward differentiation formula (BDF2) to approximate the temporal derivative to achieve a fully discrete infinity system. To solve the resulting fully discrete systems, we develop a unified framework that is applicable to the discretization of both local and nonlocal problems. A key ingredient is to derive Dirichlet-to-Neumann (DtN)-type absorbing boundary conditions (ABCs). To do so, we apply the z-transform and solve an exterior problem using an iteration technique to derive a Dirichlet-to-Dirichlet (DtD)-type mapping as exact ABCs. After that, we use the Green formula to reformulate the DtD-type mapping equivalently as the DtN-type mapping. The resulting DtN-type mapping allows us to reduce the infinity discrete system into a finite discrete system in a truncated computational domain of interest, and also make it possible to present the stability and convergence analysis of the reduced problem under some open but reasonable assumptions. To efficiently implement the exact ABCs, we further develop a fast convolution algorithm based on approximation of the contour integral induced by the inverse z-transform. The stability and error analysis of the reduced finite discrete system based on the fast algorithm for exact ABCs are also established, and numerical examples are provided to demonstrate the effectiveness of our proposed approach.

**Key words.** nonlocal diffusion equation, asymptotically compatible, artificial boundary method, absorbing boundary conditions, fast algorithm, stability and error analysis, DtN-type map

 $\textbf{AMS subject classifications.} \ 82C21, \ 65R20, \ 65M60, \ 46N20, \ 45A05$ 

**DOI.** 10.1137/19M1285822

1. Introduction. Conventional heat (diffusion) equations representing a class of partial differential equations have been applied to many fields [1] such as heat transfer, fluid dynamics, astrophysics, and finance. Nonlocal diffusion models given

<sup>\*</sup>Received by the editors September 12, 2019; accepted for publication (in revised form) April 3, 2020; published electronically June 22, 2020.

https://doi.org/10.1137/19M1285822

Funding: The work of the first author was partially supported by the National Natural Science Foundation of China grant 11771248 and the Natural Science Foundation of Xinjiang Autonomous Region grant 2019D01C026. The work of the second author was partially supported by the National Science Foundation grant DMS-1719699, the AFOSR MURI Center for Material Failure Prediction through Peridynamics, and the ARO MURI grant W911NF-15-1-0562 on Fractional PDEs for Conservation Laws and Beyond: Theory, Numerics and Applications. The work of the fourth author was partially supported by the National Natural Science Foundation of China grant 11771035, the NSAF grant U1930402, the Natural Science Foundation of Hubei Province grant 2019CFA007, and the Xiangtan University grant 2018ICIP01.

<sup>&</sup>lt;sup>†</sup>College of Mathematics and Systems Science, Xinjiang University, Urumqi 830046, China, and Department of Mathematical Sciences, Tsinghua University, Beijing 100084, China (czheng@tsinghua.edu.cn).

<sup>&</sup>lt;sup>‡</sup>Department of Applied Physics and Applied Mathematics, and Data Science Institute, Columbia University, New York, NY 10027 (qd2125@columbia.edu).

<sup>§</sup>Department of Mathematical Sciences, Tsinghua University, Beijing 100084, China (ma-x15@ mails.tsinghua.edu.cn).

<sup>¶</sup>School of Mathematics and Statistics, and Hubei Key Laboratory of Computational Science, Wuhan University, Wuhan 430072, China (jwzhang@whu.edu.cn).

in terms of integral equations can be viewed as more general models than the local diffusion equations [8]. In this paper, we develop an efficient numerical scheme for local heat/diffusion equations on unbounded spatial domains:

(1.1) 
$$(\partial_t + \mathcal{L}_0)q(x,t) = 0, \quad (x,t) \in \mathbb{R} \times (0,T],$$
$$q(x,0) = \varphi(x), \quad x \in \mathbb{R},$$
$$\lim_{x \to \pm \infty} q(x,t) = 0, \quad t \in (0,T],$$

and nonlocal heat/diffusion equations:

(1.2) 
$$(\partial_t + \mathcal{L}_{\delta})q(x,t) = 0, \quad (x,t) \in \mathbb{R} \times (0,T],$$
$$q(x,0) = \varphi(x), \quad x \in \mathbb{R},$$
$$\lim_{x \to +\infty} q(x,t) = 0, \quad t \in (0,T],$$

where the initial value  $\varphi$  is a given compactly supported function (see more discussion on  $\varphi$  in section 2.3), the local operator  $\mathcal{L}_0$  is defined as (1.5), and the nonlocal operator  $\mathcal{L}_{\delta}$  is a linear integral operator defined as

(1.3) 
$$\mathcal{L}_{\delta}q(x) = \int_{\mathbb{R}} [q(x) - q(y)] \gamma \left( y - x, \frac{y + x}{2} \right) dy.$$

The (interaction) kernel function  $\gamma$  in (1.3) has the following properties:

- nonnegativeness:  $\gamma(\alpha, \beta) \geq 0$ ;
- symmetry in  $\alpha$ :  $\gamma(-\alpha, \beta) = \gamma(\alpha, \beta)$ ;
- finite horizon:  $\exists \delta > 0$  such that  $\gamma(\alpha, \beta) = 0$  if  $|\alpha| > \delta > 0$ .

The nonlocal operator  $\mathcal{L}_{\delta}$  has an intimate connection with local differential operators. Specifically, if the kernel function  $\gamma$  satisfies the moment condition

(1.4) 
$$0 < \sigma(x) = \frac{1}{2} \int_{\mathbb{R}} s^2 \gamma \left( s, x + \frac{s}{2} \right) ds < \infty,$$

then the nonlocal operator  $\mathcal{L}_{\delta}$  converges to the second-order differential operator; see [8, 9, 11, 40], namely

(1.5) 
$$\lim_{\delta \to 0} \mathcal{L}_{\delta} q(x) = -\partial_x (\sigma(x)\partial_x) q(x) := \mathcal{L}_0 q(x).$$

Such consistency is quite useful not only for the modeling, but also the validation/verification of numerical simulations. The asymptotic compatibility (AC) scheme, a concept developed in [31, 32] and further extended in [33], is introduced to discretize the nonlocal operator to preserve such an (analogous) limit (1.5) on the discrete level.

The AC scheme can guarantee that numerical solutions are consistent with both the corrected local limiting problem  $(\delta \to 0)$  and nonlocal problem  $(\delta = \mathcal{O}(1))$ .

For problems defined on unbounded domains, one of the popular tools is the artificial boundary method (ABM); see monograph [18] and review papers [13, 15, 34]. The key process of ABM is the construction of suitable artificial/absorbing boundary conditions (ABCs). While the ABCs for local heat equations [14, 16, 17, 25, 35, 36, 38], Schrödinger equations [3, 4, 19, 20, 21, 25, 29], and wave equations [2, 24] have been well studied, only a relative few works have focused on the nonlocal problems [37, 39, 10, 11]. For nonlocal heat equations, the construction of nonlocal ABCs is generally implemented in a layer due to the nonlocal interaction, which leads to the

additional complications in both implementation and in the analysis of stability and convergence of the resulting reduced problem on the bounded computational domain.

The aim of this paper is to present a unified framework to efficiently develop a fast, stable, and second-order scheme, which is suitable for both local and nonlocal diffusion equations on unbounded spatial domains. To this end, we first introduce spatial discretizations, based on the central difference scheme and the asymptotic compatibility (AC) scheme, to discretize the heterogeneous local derivative operator and nonlocal diffusion operator, respectively, and use the second-order backward differentiation formula (BDF2) to discretize the temporal derivative. After that, we apply the z-transform to the exterior problem for the resulting infinite-dimensional system, which is assumed to be well-posed. By the iteration technique to solve a second-order operator difference equation, we obtain the exact Dirichlet-to-Dirichlet (DtD)-type mapping from artificial boundary points to ghost points. We then use the discrete Green formula to reformulate the DtD-type mapping into a Dirichlet-to-Neumann (DtN)-type mapping. Taking the DtN mapping as our ABCs, we finally obtain a reduced problem on a bounded computational domain of interest. The DtNtype ABCs lead us to the corresponding stability and convergence analysis for the proposed scheme, under some additional assumptions on the sectorial properties of related linear operators, the special kernels considered in this paper. The latter remains an open question to be studied beyond the current work.

In fact, for the resulting ABCs that contain temporal convolution induced by the inverse z-transform, the estimates on computational cost and the analysis of numerical stability and error analysis for numerical methods have been challenging even for local PDEs [3, 20, 29]. Nevertheless, it is important to point out that the iteration technique used in the design of DtD-type mapping and the Green formula to reformulate DtD-type mapping into DtN-type are available whatever the system that arises from the discretization of local or nonlocal models.

To reduce the computational cost for long time or small time-step simulations, we consider the fast evaluation of temporal convolution. In the literature, fast algorithms are well studied by utilizing the summation of exponentials to approximate the convolution kernel. One can see the derivation of exponentials through quadrature approximation in the time domain [4, 19, 38], direct rational approximation of kernel symbols [2], or quadrature approximation of contour integrals in the Laplace domain [21, 24]. In this paper, we use the main idea in [22, 23, 27, 28] to present a fast evaluation of the temporal convolution for the boundary conditions. Based on the construction of DtN-type mapping, the stability and error analysis of the resulting scheme with our fast numerical approximation is also established.

The outline of the paper is as follows. In section 2, a fully discrete local and nonlocal diffusion system is constructed, and the generalized DtN-type ABCs are derived. To reduce the computational cost, in section 3, a fast convolution algorithm is developed based on the approximation of the contour integral. The stability and error analysis is given in section 4 and numerical experiments are provided in section 5 to demonstrate the effectiveness of our approach.

## 2. Design of absorbing boundary conditions.

**2.1. Fully discrete scheme.** Let  $\{x_n\}$  be a sequence of grid points with an equidistant grid size h, and let  $\Psi_m$  be the hat basis function of width h centered at point  $x_m$ . For the discretizaiton of local operator (1.5), the second-order central

difference scheme is given by

(2.1) 
$$\mathcal{L}_{0,h}q(x_n) = \sigma_{n+\frac{1}{2}} \frac{q(x_n) - q(x_{n+1})}{h^2} + \sigma_{n-\frac{1}{2}} \frac{q(x_n) - q(x_{n-1})}{h^2}$$
$$= \sum_{m \in \mathbb{Z}} a_{n,m} [q(x_n) - q(x_m)]$$

with

(2.2) 
$$a_{n,m} = \begin{cases} \sigma_{n+\frac{1}{2}}/h^2, & m = n+1, \\ \sigma_{n-\frac{1}{2}}/h^2, & m = n-1, \\ 0 & \text{others.} \end{cases}$$

The AC scheme proposed in [11] to discretize the general nonlocal operator  $\mathcal{L}_{\delta}$  is given as

(2.3) 
$$\mathcal{L}_{\delta,h}q(x_n) = \sum_{m \in \mathbb{Z}} a_{n,m} \left[ q(x_n) - q(x_m) \right],$$

where

(2.4) 
$$a_{n,m} = \begin{cases} \frac{1}{(n-m)h} \int_{\mathbb{R}} \Psi_{(n-m)h}(s) s \gamma\left(s, \frac{x_n + x_m}{2}\right) ds, & m \neq n, \\ 0, & m = n. \end{cases}$$

Obviously, it holds that  $a_{n,m} \geq 0$ ,  $a_{n,m} = a_{m,n}$ ,  $n, m \in \mathbb{Z}$  for both local and nonlocal problems, which implies that the operators  $\mathcal{L}_{0,h}$  and  $\mathcal{L}_{\delta,h}$  are symmetric and nonnegative. The scheme extends earlier constructions in [31] for translation invariant kernels. As shown in [11], the nonlocal coefficients in (2.3) will converge to the local coefficients in (2.1) as the nonlocal interaction  $\delta$  vanishes. Without loss of generality, we will use the notation (2.3) to represent the general case for local and nonlocal coefficients.

Let  $\tau$  be the time step, and let  $t_n = n\tau$  be the time points. The numerical approximation of  $q(x_k, t_n)$  will be denoted by  $q_k^{(n)}$ . The BDF2 discretization operator is defined by

$$\mathcal{D}_{\tau}q_k^{(n)} = \frac{3q_k^{(n)} - 4q_k^{(n-1)} + q_k^{(n-2)}}{2\tau}.$$

Applying the BDF2 time discretization and the discrete local and nonlocal operator  $\mathcal{L}_{\delta,h}$ , we have the fully discrete diffusion system:

(2.5) 
$$\mathcal{D}_{\tau}q_k^{(n)} + \mathcal{L}_{\delta,h}q_k^{(n)} = 0, \quad k \in \mathbb{Z}, \quad n \ge 2,$$
$$q_k^{(0)} = \varphi(x_k), \quad k \in \mathbb{Z},$$
$$\lim_{k \to \pm \infty} q_k^{(n)} = 0, \quad n \ge 0.$$

**2.2. The z-transform.** To streamline the notation, given a bounded infinite sequence  $\{q^{(n)}\}_{n=0}^{+\infty}$ , we define its z-transform as

$$\hat{q}(z) = \sum_{n=0}^{+\infty} z^n q^{(n)}, \quad |z| < 1,$$

and the inverse z-transform as

$$q^{(n)} = \frac{1}{2\pi i} \int_{S_{\rho}} \hat{q}(z) z^{-(n+1)} dz, \quad n > 0, \quad 0 < \rho < 1,$$

where  $S_{\rho}$  represents a circle with radius  $\rho$ .

- **2.3. DtD-type absorbing boundary conditions.** We now resort to the artificial boundary method to design ABCs for the infinite discrete system (2.5). To do so, we make some additional assumptions on the initial function  $\varphi$  and kernel function  $\gamma$  as follows:
  - $\varphi$  is compactly supported over a finite interval, say  $[x_-, x_+]$ ;
  - $\gamma$  is compactly supported over a strip  $[-\delta, \delta] \times \mathbb{R}$  with  $\delta < (x_+ x_-)/2$ ;
  - $\bullet$   $\gamma$  becomes homogeneous in the exterior domains, namely,

(2.6) 
$$\gamma(\alpha,\beta) = \gamma_L(\alpha), \quad \beta \in (-\infty, x_- + \delta], \\ \gamma(\alpha,\beta) = \gamma_R(\alpha), \quad \beta \in [x_+ - \delta, +\infty).$$

The functions  $\gamma_L$  and  $\gamma_R$  can be different. For the sake of brevity, we assume  $\gamma_L = \gamma_R = \gamma_\infty$  in what follows. For the local problem, we only assume that the diffusion coefficient  $\sigma$  is a positive constant outside of computational domains  $\Omega$ . Let  $N_l$  be the largest integer with  $x_{N_l} \leq x_-$ , and  $N_r$  the smallest integer with  $x_+ \leq x_{N_r}$ .

We set

(2.7) 
$$L = \begin{cases} 1 & \text{local problem,} \\ \lceil \delta/h \rceil & \text{nonlocal problem} \end{cases}$$

and introduce the following notation:

$$\Omega = [N_l, N_r] \cap \mathbb{Z}, \quad \Omega^c = \mathbb{Z} \backslash \Omega, \quad \Omega^+ = [N_l - L + 1, N_r + L] \cap \mathbb{Z},$$
  

$$\Omega^r = [N_r - L + 1, N_r] \cap \mathbb{Z}, \quad \Omega^{r,c} = [N_r + 1, +\infty) \cap \mathbb{Z},$$
  

$$\Omega^l = [N_l, N_l + L - 1] \cap \mathbb{Z}, \quad \Omega^{l,c} = (-\infty, N_l - 1] \cap \mathbb{Z}.$$

Note that by definition if  $\delta/h$  is an integer, then  $\lceil \delta/h \rceil = \delta/h$ . Based on the above assumptions on  $\varphi$  and  $\gamma$  in nonlocal problems, we conclude that

$$q_k^{(0)} = 0$$
,  $k \in \Omega^c$  and  $a_{n,m} = -c_{n-m}$ ,  $n \in \Omega^c$ ,  $m \in \mathbb{Z}$ ,

where

(2.8) 
$$c_k = \begin{cases} -\frac{1}{kh} \int_{\mathbb{R}} \Psi_{kh}(s) s \gamma_{\infty}(s) ds, & k \neq 0, \\ -\sum_{m \neq 0} c_m, & k = 0. \end{cases}$$

It is clear that  $c_k = c_{-k}$ . Moreover, we know  $c_k = 0$  for all k with |k| > L. For the local problem, we have

(2.9) 
$$c_k = \begin{cases} -\sigma/h^2, & |k| = 1, \\ 2\sigma/h^2, & k = 0. \end{cases}$$

To introduce our construction of DtN-type mappings for the discrete diffusion system, we first consider the right homogeneous subproblem, namely,

(2.10) 
$$\mathcal{D}_{\tau}q_{k}^{(n)} + \sum_{m=-L}^{L} c_{m}q_{k+m}^{(n)} = 0, \quad k \in \Omega^{r,c}, \quad n \geq 2,$$
$$q_{k}^{(0)} = 0, \qquad k \in \Omega^{r,c},$$
$$\lim_{k \to +\infty} q_{k}^{(n)} = 0, \quad n \geq 0.$$

Performing the z-transform on both sides of (2.10), we obtain

(2.11) 
$$s\hat{q}_k + \sum_{m=-L}^{L} c_m \hat{q}_{k+m} = 0, \quad k \in \Omega^{r,c},$$
$$\lim_{k \to +\infty} \hat{q}_k = 0,$$

where

$$(2.12) s = (3 - 4z + z^2)/(2\tau).$$

It is easy to verify that the principal square root of (2.12) is

$$(2.13) z = 2 - \sqrt{1 + 2\tau s}.$$

We introduce a bounded sequence space in  $\ell^2$ -norm:

$$\mathbf{l}_0 = \{ q = \{ q_k \}_{k \in \mathbb{Z}} : \#q < +\infty \},$$

where the symbol # stands for the number of nonzero elements. Let us define the linear operator  $\mathcal{T}$  which acts on  $\mathbf{l}_0$  as

$$\mathcal{T}q = \left\{ \sum_{m=-L}^{L} c_m q_{k+m} \right\}_{k \in \mathbb{Z}} \quad \forall q = \{q_k\}_{k \in \mathbb{Z}} \in \mathbf{l}_0.$$

It is obvious to verify that the operator  $\mathcal{T}$  is symmetric and nonnegative definite. Therefore,  $\varrho(\mathcal{T})$ , the spectrum of  $\mathcal{T}$ , lies on the right half real axis [11].

Denote

(2.14) 
$$\hat{\mathbf{Q}}_{r,k} = [\hat{q}_{N_r+(k-1)L+1}, \hat{q}_{N_r+(k-1)L+2}, \dots, \hat{q}_{N_r+kL}]^T.$$

We can rewrite the fully discrete diffusive problem (2.11) into a second-order matrix (or scalar for local problem) difference equation:

(2.15) 
$$s\hat{\mathbf{Q}}_{r,k} + A\hat{\mathbf{Q}}_{r,k-1} + B\hat{\mathbf{Q}}_{r,k} + A^T\hat{\mathbf{Q}}_{r,k+1} = 0, \quad k \ge 1,$$

$$(2.16) \hat{\mathbf{Q}}_{r,k} \to 0, \quad k \to +\infty,$$

with

$$(2.17) A = \begin{pmatrix} c_L & \cdots & c_2 & c_1 \\ & c_L & \cdots & c_2 \\ & & c_L & \cdots & c_2 \\ & & & \ddots & \ddots \\ & & & & c_L \end{pmatrix}, B = \begin{pmatrix} c_0 & c_1 & \cdots & c_{L-1} \\ c_1 & c_0 & c_1 & \cdots & c_{L-1} \\ \cdots & c_1 & c_0 & c_1 & \cdots \\ \cdots & c_1 & c_0 & c_1 & \cdots \\ c_{L-1} & \cdots & c_1 & c_0 \end{pmatrix}.$$

In the above, the coefficients  $c_k$  are defined as (2.9) for the local problem and (2.8) for the nonlocal problem, respectively. Equation (2.15) is equivalently reformulated into

(2.18) 
$$\hat{\mathbf{Q}}_{r,k} = A_0 \hat{\mathbf{Q}}_{r,k-1} + B_0 \hat{\mathbf{Q}}_{r,k+1}, \quad k \ge 1,$$

with 
$$A_0 = -(s+B)^{-1} A$$
,  $B_0 = -(s+B)^{-1} A^T$ .

With prescribed  $\hat{\mathbf{Q}}_{r,0}$  for all  $s \notin \varrho(-\mathcal{T})$ , the matrix (scalar) difference problem (2.18) admits a unique solution. By using the fast algorithm for the second-order operator difference equation developed in [11, Appendix], the value of  $\hat{\mathbf{Q}}_{r,1}$  is uniquely determined by the value of  $\hat{\mathbf{Q}}_{r,0}$  in a linear manner, namely,

$$\hat{\mathbf{Q}}_{r,1} = \hat{\mathcal{K}}(s)\hat{\mathbf{Q}}_{r,0},$$

where  $\hat{\mathcal{K}}(s)$  is an exact convolution kernel. For the local problem, we have the exact formula

(2.20) 
$$\hat{\mathcal{K}}(s) = \frac{2 + h^2 s - \sqrt{4h^2 s + h^4 s^2}}{2}.$$

For any prescribed  $s \notin \varrho(-\mathcal{T})$ , we apply the inverse z-transform to the operator  $\hat{\mathcal{K}}(s)$  to have

(2.21) 
$$K_{j} = \frac{1}{2\pi i} \int_{|z|=\rho} \frac{\hat{\mathcal{K}}(s)}{z^{j+1}} dz, \quad 0 < \rho < 1, \quad j \ge 0,$$

where  $s = (3 - 4z + z^2)/(2\tau)$ . Performing inverse z-transform to (2.19) yields

(2.22) 
$$\mathbf{Q}_{r,1}^{(n)} = \mathcal{K} * \mathbf{Q}_{r,0}^{(n)} = \sum_{m=0}^{n} K_{n-m} \mathbf{Q}_{r,0}^{(m)}, \quad n \ge 0,$$

where  $\mathbf{Q}_{r,k}^{(n)}$  represents the inverse z-transform of  $\hat{\mathbf{Q}}_{r,k}$  defined as (2.14), i.e.,

(2.23) 
$$\mathbf{Q}_{r,k}^{(n)} = [q_{N_r+(k-1)L+1}^{(n)}, q_{N_r+(k-1)L+2}^{(n)}, \dots, q_{N_r+kL}^{(n)}]^T.$$

One can see that the expression (2.22) is a DtD-type mapping. Similarly, setting

$$\hat{\mathbf{Q}}_{l,k} = [\hat{q}_{N_l - (k-1)L - 1}, \hat{q}_{N_l - (k-1)L - 2}, \dots, \hat{q}_{N_l - kL}]^T,$$

$$\mathbf{Q}_{l,k}^{(n)} = [q_{N_l-(k-1)L-1}^{(n)}, q_{N_l-(k-1)L-2}^{(n)}, \dots, q_{N_l-kL}^{(n)}]^T$$

and considering the left homogeneous subproblem, we have the left DtD-type mapping as

(2.24) 
$$\mathbf{Q}_{l,1}^{(n)} = \mathcal{K} * \mathbf{Q}_{l,0}^{(n)} = \sum_{m=0}^{n} K_{n-m} \mathbf{Q}_{l,0}^{(m)}, \quad n \ge 0.$$

Taking DtD-type mappings (2.22) and (2.24) as ABCs, we have the discrete system on the truncated domain:

(2.25) 
$$\mathcal{D}_{\tau}q_{k}^{(n)} + \mathcal{L}_{\delta,h}q_{k}^{(n)} = 0, \quad k \in \Omega, \quad n \geq 2,$$

$$\mathbf{Q}_{r,1}^{(n)} = \sum_{m=0}^{n} K_{n-m}\mathbf{Q}_{r,0}^{(m)}, \quad \mathbf{Q}_{l,1}^{(n)} = \sum_{m=0}^{n} K_{n-m}\mathbf{Q}_{l,0}^{(m)},$$

$$q_{k}^{(1)} = q_{k}^{(0)} + \tau \partial_{t}q_{k}^{(0)} = \varphi(x_{k}) + \tau \mathcal{L}_{\delta,h}\varphi(x_{k}), \quad k \in \Omega,$$

$$q_{k}^{(0)} = \varphi(x_{k}), \quad k \in \Omega^{+}.$$

2.4. DtN-type absorbing boundary conditions. It is well known that Neumann type problems substantially differ from the Dirichlet type problems for nonlocal/fractional equations; see [6, 7, 9, 12, 30]. The study of Neumann problems will have an important influence on many applications such as interface problems, free boundary problems, and domain compositions of nonlocal problems. We consider here the Neumann data based on the definition of the discrete operator. By the discrete Green formula, we have

$$\sum_{n \in \Omega} \mathcal{L}_{\delta,h} q_n \cdot v_n = \sum_{n \in \Omega} \sum_{m \in \Omega} a_{n,m} (q_n - q_m) v_n + \sum_{n \in \Omega} \sum_{m \in \Omega^c} a_{n,m} (q_n - q_m) v_n$$

$$= \frac{1}{2} \sum_{n \in \Omega} \sum_{m \in \Omega} a_{n,m} (q_n - q_m) (v_n - v_m) + \sum_{n \in \Omega} \sum_{m \in \Omega^c} a_{n,m} (q_n - q_m) v_n$$

$$= \frac{1}{2} \sum_{n \in \Omega} \sum_{m \in \Omega} a_{n,m} (q_n - q_m) (v_n - v_m) + \sum_{n \in \Omega} \sum_{m \in \Omega^c} a_{n,m} (q_n - q_m) (v_n - v_m)$$

$$(2.26) - \sum_{n \in \Omega^c} \sum_{m \in \Omega} a_{n,m} (q_n - q_m) v_n.$$

From (2.26), we formulate the interior and exterior Neumann data, respectively, as

(2.27) 
$$\mathcal{N}_{\Omega}q_n = -\sum_{m \in \Omega^c} a_{n,m}(q_n - q_m), \quad n \in \Omega,$$

(2.28) 
$$\mathcal{N}_{\Omega^c} q_n = \sum_{m \in \Omega} a_{n,m} (q_n - q_m), \quad n \in \Omega^c.$$

We point out that the interior and exterior Neumann data are useful for the proofs of Theorem 4.1 and Lemma 4.1.

Noting that the discrete coefficients satisfy  $a_{n,m} = -c_{n-m}$  on artificial layers, we may rewrite (2.27) into

(2.29) 
$$\mathcal{N}_{\Omega}q_n = \sum_{m \in \Omega^c} c_{n-m}q_n - \sum_{m \in \Omega^c} c_{n-m}q_m, \quad n \in \Omega^r.$$

Prescribed  $\mathbf{Q}_{r,0}$ , we can address (2.29) in the form of a vector as

(2.30) 
$$\mathcal{N}_{\Omega} \mathbf{Q}_{r,0} = D \mathbf{Q}_{r,0} - A^T \mathbf{Q}_{r,1},$$

where the matrix A is given in (2.17) and

$$D = \text{diag}\left(\sum_{i=L}^{L} c_{i}, \sum_{i=L-1}^{L} c_{i}, \dots, \sum_{i=1}^{L} c_{i}\right).$$

Similarly, for the DtD-type mappings (2.24), we have

(2.31) 
$$\mathcal{N}_{\Omega} \mathbf{Q}_{l,0} = D \mathbf{Q}_{l,0} - A^T \mathbf{Q}_{l,1}.$$

The corresponding Green formula (2.32) is given as

(2.32) 
$$\sum_{n \in \Omega} \mathcal{L}_{\delta,h} q_n \cdot v_n = \frac{1}{2} \sum_{n \in \Omega} \sum_{m \in \Omega} a_{n,m} (q_n - q_m) (v_n - v_m) - \mathcal{N}_{\Omega} \mathbf{Q}_{l,0} \cdot \mathbf{V}_{l,0} - \mathcal{N}_{\Omega} \mathbf{Q}_{r,0} \cdot \mathbf{V}_{r,0},$$

where

$$\begin{aligned} \mathbf{V}_{r,0}^{(n)} &= [v_{N_r-L+1}^{(n)}, v_{N_r-L+2}^{(n)}, \dots, v_{N_r}^{(n)}]^T, \\ \mathbf{V}_{l,0}^{(n)} &= [v_{N_l+L-1}^{(n)}, v_{N_l+L-2}^{(n)}, \dots, v_{N_l}^{(n)}]^T. \end{aligned}$$

Applying the relationships (2.22) and (2.24) to (2.30) and (2.31), we have the following truncated problem with DtN-type mappings:

(2.33) 
$$\mathcal{D}_{\tau}q_{k}^{(n)} + \mathcal{L}_{\delta,h}q_{k}^{(n)} = 0, \quad k \in \Omega, \quad n \geq 2,$$

$$\mathcal{N}_{\Omega}\mathbf{Q}_{r,0}^{(n)} = (D - A^{T}\mathcal{K}*)\mathbf{Q}_{r,0}^{(n)}, \quad \mathcal{N}_{\Omega}\mathbf{Q}_{l,0}^{(n)} = (D - A^{T}\mathcal{K}*)\mathbf{Q}_{l,0}^{(n)},$$

$$q_{k}^{(1)} = q_{k}^{(0)} + \tau\partial_{t}q_{k}^{(0)} = \varphi(x_{k}) + \tau\mathcal{L}_{\delta,h}\varphi(x_{k}), \quad k \in \Omega,$$

$$q_{k}^{(0)} = \varphi(x_{k}), \quad k \in \Omega^{+}.$$

- 3. Fast convolution algorithm. Because the DtD-type mappings in (2.25) and the DtN-type mappings in (2.33) involve the temporal convolutions, computational cost and storage will be formidable for long-time or small time-step simulations. In this section, we focus on developing a fast algorithm to significantly reduce the computational cost and storage to evaluate ABCs.
- **3.1. Quadrature error analysis.** To develop a fast algorithm for our DtN-type ABCs, the key point is to construct an efficient numerical approximation of the inverse z-transform of  $\hat{\mathcal{K}}(s)$  with certain holomorphic mappings. Here we use the discretized contour integrals developed in [22, 23, 27, 28] for the inverse Laplace transform. The technique in [19] is based on the assumption that the matrix-valued symbol  $\hat{\mathcal{K}}(s)$  is sectorial, namely, it satisfies

(3.1) 
$$\|\hat{\mathcal{K}}(s)\|_2 \le \frac{M}{|s|} \quad \text{for} \quad |\arg(s)| < \pi - \psi \quad \text{with} \quad 0 < \psi < \frac{1}{2}\pi,$$

and the integration contour  $\Gamma_s$  may then be changed as

(3.2) 
$$\mathbb{R} \to \Gamma_s : \theta \longmapsto \gamma_s(\theta) = \mu(1 - \sin(\alpha + i\theta)) + \sigma,$$

where  $\mu$  represents a positive scale parameter,  $\alpha$  ( $<\pi/2$ ) is a positive angle, and  $\sigma$  represents a shift parameter. One can see a graphical illustration of a contour  $\Gamma_s$  in Figure 1 for given parameters  $\mu = 1$ ,  $\alpha = \pi/4$ , and  $\sigma = 0$ .

According to (2.20) for the local problem, one can check that  $\hat{\mathcal{K}}(s)$  satisfies the condition (3.1). Unfortunately, at the moment the assumption on the sectorial property remains to be verified for the nonlocal problem but we will proceed with our analysis based on its validity.

After parametrizing (2.21) via  $\gamma_s(\theta)$  (s is defined in (2.12)), we get

(3.3) 
$$K_j = \frac{1}{2\pi} \int_{-\infty}^{+\infty} G_j(\theta) d\theta,$$

where

(3.4) 
$$G_j(\theta) = \frac{\hat{\mathcal{K}}(\gamma_s(\theta))}{\left(2 - \sqrt{1 + 2\tau\gamma_s(\theta)}\right)^{j+1}} \frac{\mu\tau\cos(\alpha + i\theta)}{\sqrt{1 + 2\tau\gamma_s(\theta)}}.$$

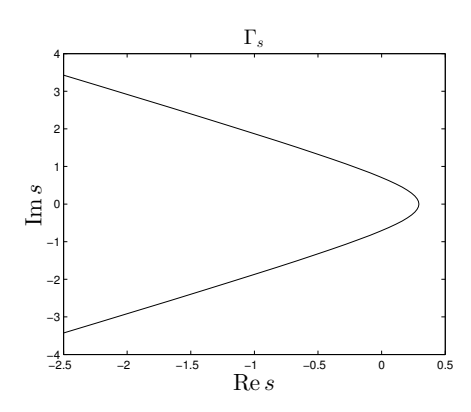


Fig. 1. Sketch map of the contours  $\Gamma_s$  with  $\mu = 1$ ,  $\alpha = \pi/4$ , and  $\sigma = 0$ .

Apply the truncated trapezoidal rule (see [23]) to approximate the contour integral (3.3). We then arrive at

(3.5) 
$$K_j \approx \frac{\tilde{\tau}}{2\pi} \sum_{n=-N}^{N} G_j(\theta_n) \equiv \tilde{K}_j,$$

where  $\theta_n = n\tilde{\tau}$  and  $\tilde{\tau}$  represents a step length parameter of the trapezoidal rule for the contour integral.

Our following analysis is similar to the error analyses of the trapezoidal rule for the holomorphic integrands [22, 23, 27, 28]. In the spirit of [22, section 6], we recall the conformal mapping

(3.6) 
$$\gamma_s(\theta) = \mu(1 - \sin(\alpha + i\theta)).$$

Let us select  $\alpha, d > 0$  such that  $0 < \alpha - d < \alpha + d < \pi/2 - \psi$ . The mapping  $\gamma_s$  (3.6) transforms each horizontal straight line Im  $\theta = \beta$ ,  $-d \le \beta \le d$  into a left branch of the hyperbola

$$\lambda \in \mathbb{C}: \ \left(\frac{\mathrm{Re}\lambda - \mu}{\mu \mathrm{sin}(\alpha - \beta)}\right)^2 - \left(\frac{\mathrm{Im}\lambda}{\mu \mathrm{cos}(\alpha - \beta)}\right)^2 = 1$$

with the foci at  $(0,0), (2\mu,0)$  and asymptotes forming angles  $\pm [\pi/2 - (\alpha - \beta)]$ . Therefore,  $\gamma_s$  transforms the horizontal strip  $D_d = \{\theta \in \mathbb{C} : |\text{Im }\theta| \leq d\}$  into the region  $\Omega = \gamma_s(D_d)$  which is limited by the left branches corresponding to  $\beta = \pm d$ . Noting (3.1) and assuming that  $\alpha > 0$  and d > 0 with  $0 < \alpha - d < \alpha + d < \pi/2 - \psi$ , we have all the hyperbolas lie in the sector of analyticity of  $\hat{\mathcal{K}}(s)$ .

We now aim to obtain the quadrature error of the following truncated trapezoidal rule (3.5) for the integral of  $G_i$ :

(3.7) 
$$E_{\tilde{\tau},N}(G_j) = \frac{1}{2\pi} \int_{-\infty}^{+\infty} G_j(\theta) d\theta - \frac{\tilde{\tau}}{2\pi} \sum_{n=-N}^{N} G_j(n\tilde{\tau}), \quad \tilde{\tau} > 0, \quad N \ge 1.$$

To estimate  $E_{\tilde{\tau},N}(G_i)$ , we use the same methodology developed in [22, 23]. The

mapping  $G_j$  satisfies the following two conditions:

$$\int_{-d}^{d} \|G_j(\theta + i\beta)\|_2 d\beta \to 0 \quad \text{as} \quad |\theta| \to +\infty,$$

$$N(G_j, D_d) := \int_{-\infty}^{+\infty} \|G_j(\theta + id)\|_2 + \|G_j(\theta - id)\|_2 d\theta < +\infty.$$

Without loss of generality, we set parameters for the following analysis and simulations as

$$\sigma = 0$$
,  $\alpha = \frac{\pi}{4}$ ,  $\psi = \frac{\pi}{24}$ ,  $d = \frac{\pi}{6}$ ,  $B = 10$ ,  $k_0 = 20$ .

Using the similar techniques as in [22, 23], we have the following results stated in Lemmas 3.1–3.3 and Theorem 3.1. For brevity, we leave the proofs of these results to the appendix. Differing from the proofs in [22, 23], we divide the whole integral interval into two parts, and obtain the proper upper bounds, respectively.

Lemma 3.1. Let  $|\beta| \le d$ ,  $\theta \ge \ln(56/(\mu\tau) + 2)$ ,  $\mu\tau \le 1$ ,  $k \ge 1$ , and  $t = k\tau$ . It holds that

$$||G_k(\theta + i\beta)||_2 \le \frac{M_0}{(1 - \mu t/k)^{\frac{k+1}{2}}} \left(1 + \frac{\mu t}{k} \cosh \theta\right)^{-\frac{k+1}{2}},$$

where  $M_0 = 2M\tau\sqrt{\frac{1+\sin(\alpha+d)}{1-\sin(\alpha-d)}}$ , and  $G_k$  is defined as (3.4).

LEMMA 3.2. If  $R \ge 0$ , a > 0, and  $k \ge 1$ , it holds that

$$\int_{R}^{+\infty} \left( 1 + \frac{a}{k} \cosh \theta \right)^{-\frac{k+1}{2}} d\theta \le \phi(a) \exp\left( -\frac{a \cosh R}{4} \right) + \left( 1 + \frac{a}{k} \cosh R \right)^{-\frac{k-1}{2}},$$

where  $\phi(a) = 2 + |\ln(1 - \exp(-a/4))|$ .

We refer the reader to [22, Lemma 2] for the proof of Lemma 3.2.

LEMMA 3.3. If  $k \geq 1/(100\mu\tau)$ ,  $\mu\tau \leq 1/2$ , and  $N\tilde{\tau} \geq \ln(56/(\mu\tau) + 2)$ , it holds that

$$N(G_k, D_d) \leq 9M_0N\tilde{\tau}\exp(2\mu t).$$

Theorem 3.1. If  $t=k\tau$ ,  $k\geq 1/(100\mu\tau)$ ,  $\mu\tau\leq 1/2$ , and  $N\tilde{\tau}\geq \ln(56/(\mu\tau)+2)$ , it holds that

$$||E_{\tilde{\tau},N}(G_k)||_2 \leq 10M_0N\tilde{\tau}\exp\left(2\mu t - \frac{2\pi d}{\tilde{\tau}}\right) + 16\sqrt{2}M_0\exp\left(\mu t - \frac{\mu t\cosh(N\tilde{\tau})}{4}\right) + 2\sqrt{2}M_0\exp(\mu t)\left(1 + \frac{\mu t}{k}\cosh(N\tilde{\tau})\right)^{-\frac{k-1}{2}}.$$

Theorem 3.1 implies that for any given tolerance error  $\varepsilon > 0$ , the leading order of  $||E_{\tilde{\tau},N}(G_k)||_2$  is the order of  $\mathcal{O}(\varepsilon)$  if we take the parameters to satisfy

$$2\mu t - \frac{2\pi d}{\tilde{\tau}} \le \ln \varepsilon, \quad k > b \log \frac{1}{\varepsilon}, \quad \text{and} \quad \frac{1}{B} \log \frac{1}{\varepsilon} \le \mu t \le \log \frac{1}{\varepsilon},$$

where b and B > 1 are two given positive constants.

Noting that within one set of quadrature points of the contour as shown in [22], we do not have a uniformly good approximation for all  $n = 0, ..., N_T$ , where  $N_T = T/\tau$ 

represents the total number of time grid points. Thus, we locally introduce a sequence of fast-growing time index intervals

$$I_0 = [0, k_0]$$
 and  $I_m = (k_0 B^{m-1}, k_0 B^m], m \ge 1,$ 

where  $k_0$  is a given positive constant. The contour  $\Gamma_s^{(m)}$  is accordingly chosen as

(3.8) 
$$\mathbb{R} \to \Gamma_s^{(m)} : \theta \longmapsto \gamma_s^{(m)}(\theta) = \mu_m (1 - \sin(\alpha + i\theta)),$$

with an m-dependent parameter  $\mu_m = 1/(125B^m\tau) > 0$ . Recalling (3.5) and (3.4), we approximate the contour integrals (2.21) as

(3.9) 
$$\tilde{K}_j \equiv \frac{\tilde{\tau}}{2\pi} \sum_{n=-N_m}^{N_m} \omega_n^{(m)} \left( p_n^{(m)} \right)^{j+1} \approx K_j \qquad \forall j \in I_m,$$

where

(3.10) 
$$\omega_n^{(m)} = \frac{\mu_m \tau \cos(\alpha + i\theta_n) \hat{\mathcal{K}}(\gamma_s^{(m)}(\theta_n))}{\sqrt{1 + 2\tau \gamma_s^{(m)}(\theta_n)}}$$
 and  $p_n^{(m)} = \frac{1}{2 - \sqrt{1 + 2\tau \gamma_s^{(m)}(\theta_n)}}$ .

On the other hand, the approximation is poor for  $j \in I_0$ . We use the following approximate formula to directly calculate  $K_j$  while  $j \in I_0$ , namely

(3.11) 
$$\tilde{K}_{j} \equiv \frac{\rho^{-j}}{N_{0}} \sum_{n=1}^{N_{0}} \hat{\mathcal{K}}(s(e^{-2n\pi i/N_{0}}))e^{-2jn\pi i/N_{0}} \approx K_{j}, \quad j \in I_{0}.$$

Before ending this section, we point out that, for any given tolerance error  $\varepsilon > 0$  and time step  $\tau$ , we can employ the following formula for the calculation of local contours such that  $||E_{\tilde{\tau},N}(G_k)||_2 = \mathcal{O}(\varepsilon)$ , namely

(3.12) 
$$\tilde{\tau} = -\frac{2\pi d}{1.01 \ln \varepsilon}, \quad \mu_m = \frac{1}{125 B^m \tau}, \quad N_m = \ln \left(\frac{56}{\mu_m \tau} + 2\right) / \tilde{\tau}.$$

**3.2.** Numerical schemes with fast evaluation of ABCs. Replacing  $K_m$  in (2.22) and (2.24) with  $\tilde{K}_m$ , we derive the approximate mappings which can be efficiently evaluated as

(3.13) 
$$\mathbf{Q}_{r,1}^{(n)} = \tilde{\mathcal{K}} * \mathbf{Q}_{r,0}^{(n)} = \sum_{m=0}^{n} \tilde{K}_{n-m} \mathbf{Q}_{r,0}^{(m)}, \quad n \ge 0,$$

(3.14) 
$$\mathbf{Q}_{l,1}^{(n)} = \tilde{\mathcal{K}} * \mathbf{Q}_{l,0}^{(n)} = \sum_{m=0}^{n} \tilde{K}_{n-m} \mathbf{Q}_{l,0}^{(m)}, \quad n \ge 0.$$

Again, applying the relationships (3.13) and (3.14) to (2.30) and (2.31), we have the following truncated problem with fast evaluations of DtN-type mappings:

(3.15) 
$$\mathcal{D}_{\tau}q_{k}^{(n)} + \mathcal{L}_{\delta,h}q_{k}^{(n)} = 0, \quad k \in \Omega, \quad n \geq 2,$$

$$\mathcal{N}_{\Omega}\mathbf{Q}_{r,0}^{(n)} = (D - A^{T}\tilde{\mathcal{K}}*)\mathbf{Q}_{r,0}^{(n)}, \quad \mathcal{N}_{\Omega}\mathbf{Q}_{l,0}^{(n)} = (D - A^{T}\tilde{\mathcal{K}}*)\mathbf{Q}_{l,0}^{(n)},$$

$$q_{k}^{(1)} = q_{k}^{(0)} + \tau\partial_{t}q_{k}^{(0)} = \varphi(x_{k}) + \tau\mathcal{L}_{\delta,h}\varphi(x_{k}), \quad k \in \Omega,$$

$$q_{k}^{(0)} = \varphi(x_{k}), \quad k \in \Omega^{+}.$$

**3.3. Fast evaluation of DtN-type boundary conditions.** We now address the detailed implementation of the fast algorithm of the convolution in ABCs. For any fixed time index  $k \in I_l = (k_0 B^{l-1}, k_0 B^l)$ , we define

(3.16) 
$$\mathcal{F}_{l}^{n}(k) = \sum_{m=k_{0}B^{l-1}+1}^{k} \left(p_{n}^{(l)}\right)^{m+1} \mathbf{Q}_{r,0}^{(k-m)},$$

$$\mathcal{G}_{i}^{n}(k) = \sum_{m=k_{0}B^{i-1}+1}^{k_{0}B^{i}} \left(p_{n}^{(i)}\right)^{m+1} \mathbf{Q}_{r,0}^{(k-m)}, \quad 1 \leq i \leq l-1,$$

which have the recursion relations in the forms of

(3.17) 
$$\mathcal{F}_{l}^{n}(k+1) = \left(p_{n}^{(l)}\right)^{k_{0}B^{l-1}+2} \mathbf{Q}_{r,0}^{(k-k_{0}B^{l-1})} + p_{n}^{(l)}\mathcal{F}_{l}^{n}(k),$$

$$\mathcal{G}_{i}^{n}(k+1) = \left(p_{n}^{(i)}\right)^{k_{0}B^{i-1}+2} \mathbf{Q}_{r,0}^{(k-k_{0}B^{i-1})} - \left(p_{n}^{(i)}\right)^{k_{0}B^{i}+2} \mathbf{Q}_{r,0}^{(k-k_{0}B^{i})}$$

$$+ p_{n}^{(i)}\mathcal{G}_{i}^{n}(k), \quad 1 \leq i \leq l-1.$$

We take the discrete convolution (3.13) as an example, and have the similar fast evaluation for (3.14). By definition, (3.13) can be divided into l + 2 parts:

(3.19) 
$$\mathbf{Q}_{r,1}^{(k)} = \tilde{K}_0 \mathbf{Q}_{r,0}^{(k)} + \sum_{m=1}^{k_0} \tilde{K}_m \mathbf{Q}_{r,0}^{(n-m)} + \tilde{\mathbf{Q}}_1^{(k)} + \dots + \tilde{\mathbf{Q}}_l^{(k)}$$

with  $\tilde{\mathbf{Q}}_{i}^{(k)}$  defined as

$$\tilde{\mathbf{Q}}_{i}^{(k)} = \sum_{m=k_{0}B^{i-1}+1}^{k_{0}B^{i}} \tilde{K}_{m} \mathbf{Q}_{r,0}^{(n-m)} = \frac{\tilde{\tau}}{2\pi} \sum_{n=-N_{i}}^{N_{i}} \omega_{n}^{(i)} \mathcal{G}_{i}^{n}(k), \quad 1 \leq i \leq l-1,$$

$$\tilde{\mathbf{Q}}_{l}^{(k)} = \sum_{m=k_{0}B^{l-1}+1}^{k} \tilde{K}_{m} \mathbf{Q}_{r,0}^{(n-m)} = \frac{\tilde{\tau}}{2\pi} \sum_{n=-N_{l}}^{N_{l}} \omega_{n}^{(l)} \mathcal{F}_{l}^{n}(k),$$

where the coefficients  $\omega_n^{(\cdot)}$  are given in (3.10).

- 4. Stability and error analysis. We now present the stability and error estimate for the approximate fully discrete problem (3.15) with fast evaluations of DtN-type boundary conditions under the assumptions made in earlier sections.
- **4.1. Stability analysis for a nonlocal discrete system.** We first consider the stability analysis of the following discrete scheme:

$$\mathcal{D}_{\tau}\phi_k^{(n)} + \mathcal{L}_{\delta,h}\phi_k^{(n)} = f_k^{(n)}, \quad k \in \Omega, \quad n \ge 2,$$

(4.2) 
$$\mathcal{N}_{\Omega} \mathbf{\Phi}_{r,0}^{(n)} = (D - A^T \mathcal{K} *) \mathbf{\Phi}_{r,0}^{(n)} + \mathbf{G}_r^{(n)},$$

(4.3) 
$$\mathcal{N}_{\Omega} \mathbf{\Phi}_{l,0}^{(n)} = (D - A^T \mathcal{K} *) \mathbf{\Phi}_{l,0}^{(n)} + \mathbf{G}_l^{(n)}$$

(4.4) 
$$\phi_k^{(1)} = \phi_k^{(0)} + \tau \partial_t \phi_k^{(0)} + f_k^{(1)}, \quad k \in \Omega,$$

with the given initial values  $\phi_k^{(0)}$  for  $k \in \Omega^+$  and

$$\boldsymbol{\Phi}_{r,0}^{(n)} = [\phi_{N_r-L+1}^{(n)}, \phi_{N_r-L+2}^{(n)}, \dots, \phi_{N_r}^{(n)}]^T$$

$$\mathbf{\Phi}_{l,0}^{(n)} = [\phi_{N_l+L-1}^{(n)}, \phi_{N_l+L-2}^{(n)}, \dots, \phi_{N_l}^{(n)}]^T,$$

$$\mathbf{G}_r^{(n)} = \{g_{r,1}^{(n)}, \dots, g_{r,L}^{(n)}\}$$
 and  $\mathbf{G}_l^{(n)} = \{g_{l,1}^{(n)}, \dots, g_{l,L}^{(n)}\}.$ 

To do so, we introduce the inner product and the induced norm

$$\left(\phi^{(n)}, \varphi^{(n)}\right)_h = h \sum_{k \in \Omega} \phi_k^{(n)} \varphi_k^{(n)}, \quad \|\phi^{(n)}\|_h = \sqrt{(\phi^{(n)}, \phi^{(n)})_h}$$

for the vectors  $\phi^{(n)} = (\phi_k^{(n)})_{k \in \Omega}$  and  $\varphi^{(n)} = (\varphi_k^{(n)})_{k \in \Omega}$ .

LEMMA 4.1. The discrete DtN operator is stable, in the sense that for sequences  $\mathbf{V}_{*,0}^{(n)}$  satisfying  $\mathbf{V}_{*,1}^{(n)} = \mathcal{K} * \mathbf{V}_{*,0}^{(n)}$  with  $* \in \{r,l\}$  and any  $j \geq 2$ , it holds that

(4.5) 
$$\sum_{n=2}^{j} \mathcal{N}_{\Omega} \mathbf{V}_{*,0}^{(n)} \cdot \mathbf{V}_{*,0}^{(n)} \leq 0,$$

where  $\mathcal{N}_{\Omega}\mathbf{V}_{*,0}^{(n)} = (D - A^T \mathcal{K}*)\mathbf{V}_{*,0}^{(n)}$ .

*Proof.* We consider the right homogeneous exterior problem

$$\mathcal{D}_{\tau}\phi_{k}^{(n)} + \sum_{m \in \mathbb{Z}} a_{k,m} \left[ q(x_{k}) - q(x_{m}) \right] = 0, \quad k \in \Omega^{r,c}, \quad n \geq 2,$$

$$\phi^{(0)} = \phi^{(1)} = 0,$$

$$\Phi_{r,0}^{(n)} = \mathbf{V}_{r,0}^{(n)},$$

$$\lim_{k \to +\infty} \phi_{k}^{(n)} = 0, \quad n \geq 0.$$

For problems on the exterior domain, we have the coefficients  $a_{n,m} = -c_{n-m} \ge 0$  due to the assumption on the kennel function  $\gamma$  and  $\sigma$  in section 2.3. The problem (2.10) implies (2.30). Similarly, the problem (4.6) implies that

$$\mathcal{N}_{\Omega^{r,c}} \mathbf{\Phi}_{r,0}^{(n)} = (D - A^T \mathcal{K} *) \mathbf{\Phi}_{r,0}^{(n)} = (D - A^T \mathcal{K} *) \mathbf{V}_{r,0}^{(n)} = \mathcal{N}_{\Omega} \mathbf{V}_{r,0}^{(n)}$$

Taking inner production between  $\phi_k^n$  and (4.6), and using the Green formula (2.32) of the discrete operator for the exterior domain, we have

$$\sum_{k \in \Omega^{r,c}} \mathcal{D}_{\tau} \phi_{k}^{(n)} \phi_{k}^{(n)} + \frac{1}{2} \sum_{k \in \Omega^{r,c}} \sum_{m \in \Omega^{r,c}} a_{k,m} \left( \phi_{k}^{(n)} - \phi_{m}^{(n)} \right)^{2}$$

$$+ \sum_{k \in \Omega^{r,c}} \sum_{m \in \Omega^{r}} a_{k,m} \left( \phi_{k}^{(n)} - \phi_{m}^{(n)} \right)^{2}$$

$$= \sum_{k \in \Omega^{r}} \sum_{m \in \Omega^{r,c}} a_{k,m} \left( \phi_{k}^{(n)} - \phi_{m}^{(n)} \right) \phi_{k}^{(n)} = -\mathcal{N}_{\Omega} \mathbf{V}_{r,0}^{(n)} \cdot \mathbf{V}_{r,0}^{(n)}$$

Summing the index n from 2 to j over the above identity, we have

$$\sum_{n=2}^{j} \mathcal{N}_{\Omega} \mathbf{V}_{r,0}^{(n)} \cdot \mathbf{V}_{r,0}^{(n)} \leq 0,$$

where we use the property in [26, Lemma 2.2] that

$$\sum_{n=2}^{j} \sum_{k \in \Omega^{r,c}} \mathcal{D}_{\tau} \phi_k^{(n)} \phi_k^{(n)} \ge 0.$$

By considering a left homogenous exterior problem, we similarly derive (4.5).

THEOREM 4.1. Assuming the condition (3.1) is satisfied, there exists a positive constant  $\tau_0$  such that for  $\tau \leq \tau_0$  the solution of (4.1)–(4.4) satisfies the following stability estimate for  $j \geq 2$  in the cases of the local problem with  $\delta = 0$ :

$$\|\phi^{(j)}\|_h^2 \le C \left( \|\phi^{(0)}\|_h^2 + \|\phi^{(1)}\|_h^2 + \tau \sum_{n=2}^j \left( h^2 |G_r^{(n)}|^2 + h^2 |G_l^{(n)}|^2 + \|f^{(n)}\|_h^2 \right) \right),$$

and nonlocal problem with  $\delta > 0$ :

$$\|\phi^{(j)}\|_h^2 \le C \left( \|\phi^{(0)}\|_h^2 + \|\phi^{(1)}\|_h^2 + \tau \sum_{n=2}^j \left( h \|\mathbf{G}_r^{(n)}\|_2^2 + h \|\mathbf{G}_l^{(n)}\|_2^2 + \|f^{(n)}\|_h^2 \right) \right).$$

*Proof.* Taking inner production between  $\phi_k^{(n)}$  and (4.1) and applying the Green formula (2.32) of the discrete operator for the interior domain as

$$\sum_{k \in \Omega} \mathcal{L}_{\delta,h} \phi_k^{(n)} \cdot \phi_k^{(n)} = \frac{1}{2} \sum_{k \in \Omega} \sum_{m \in \Omega} a_{k,m} (\phi_k^{(n)} - \phi_m^{(n)})^2 - \mathcal{N}_{\Omega} \mathbf{\Phi}_{l,0}^{(n)} \cdot \mathbf{\Phi}_{l,0}^{(n)} - \mathcal{N}_{\Omega} \mathbf{\Phi}_{r,0}^{(n)} \cdot \mathbf{\Phi}_{r,0}^{(n)}$$

we arrive at

(4.7) 
$$\sum_{k \in \Omega} \mathcal{D}_{\tau} \phi_{k}^{(n)} \phi_{k}^{(n)} + \frac{1}{2} \sum_{k \in \Omega} \sum_{m \in \Omega} a_{k,m} (\phi_{k}^{(n)} - \phi_{m}^{(n)})^{2} \\ = \mathcal{N}_{\Omega} \mathbf{\Phi}_{r,0}^{(n)} \cdot \mathbf{\Phi}_{r,0}^{(n)} + \mathcal{N}_{\Omega} \mathbf{\Phi}_{l,0}^{(n)} \cdot \mathbf{\Phi}_{l,0}^{(n)} + \sum_{k \in \Omega} f_{k}^{(n)} \phi_{k}^{(n)}.$$

Set

$$\begin{split} x_n &:= \|\phi^{(n)}\|_h^2, \quad y_n := \|\phi^{(n)} - \phi^{(n-1)}\|_h^2, \\ z_n &= \|f^{(n)}\|_h^2, \quad b_n = \frac{1}{2} \sum_{k \in \Omega} \sum_{m \in \Omega} a_{k,m} (\phi_k^{(n)} - \phi_m^{(n)})^2, \\ d_n &= \mathcal{N}_\Omega \boldsymbol{\Phi}_{r,0}^{(n)} \cdot \boldsymbol{\Phi}_{r,0}^{(n)} + \mathcal{N}_\Omega \boldsymbol{\Phi}_{l,0}^{(n)} \cdot \boldsymbol{\Phi}_{l,0}^{(n)}. \end{split}$$

Applying the property in [5, inequality (37)], we have

(4.8) 
$$\left(\phi^{(n)}, 2\tau \mathcal{D}_{\tau}\phi^{(n)}\right)_{h} \geq \frac{3}{2}x_{n} - 2x_{n-1} + \frac{1}{2}x_{n-2} + y_{n} - y_{n-1}.$$

Applying (4.8) to (4.7), we have

$$3x_n - 4x_{n-1} + x_{n-2} \le 2(y_{n-1} - y_n) + 4h\tau(d_n - b_n) + 4\tau\sqrt{x_n z_n}.$$

Summing the index n from 2 to j and applying Lemma 4.1, we derive (4.9)

$$x_{j} \leq 3x_{1} - x_{0} + 2y_{1} - (2y_{j} + 2x_{j} - x_{j-1}) + 4h\tau \sum_{n=2}^{j} (d_{n} - b_{n}) + 4\tau \sum_{n=2}^{j} \sqrt{x_{n}z_{n}}$$

$$\leq 5x_{1} + x_{0} - (2\sqrt{x_{j}} - \sqrt{x_{j-1}})^{2} + 4h\tau \sum_{n=2}^{j} (d_{n} - b_{n}) + 4\tau \sum_{n=2}^{j} \sqrt{x_{n}z_{n}}$$

$$\leq 5x_{1} + x_{0} + 4h\tau \sum_{n=2}^{j} \left( \left( \mathbf{\Phi}_{r,0}^{(n)}, \mathbf{G}_{r}^{(n)} \right) + \left( \mathbf{\Phi}_{l,0}^{(n)}, \mathbf{G}_{l}^{(n)} \right) - b_{n} \right) + 4\tau \sum_{n=2}^{j} \sqrt{x_{n}z_{n}}.$$

(i) For the local problem, we refer the reader to [38, Lemma 2.2 and Theorem 3.1] for an analogous proof. Applying the Cauchy inequality and the discrete embedding theorem  $\|\phi^{(n)}\|_{L^{\infty}} \leq C_0(hb_n + \|\phi^{(j)}\|_h)$  to the last inequality in (4.9), we have

$$\begin{split} x_j &\leq 5x_1 + x_0 + 2\tau \sum_{n=2}^j z_n + 2\tau \sum_{n=2}^j x_n \\ &+ 4\tau \sum_{n=2}^j \left( \frac{1}{4C_0^2} |\Phi_{r,0}^{(n)}|^2 + \frac{1}{4C_0^2} |\Phi_{l,0}^{(n)}|^2 + C_0^2 h^2 |G_r^{(n)}|^2 + C_0^2 h^2 |G_l^{(n)}|^2 - hb_n \right) \\ &\leq 5x_1 + x_0 + 4C_0^2 h^2 \tau \sum_{n=2}^j \left( |G_r^{(n)}|^2 + |G_l^{(n)}|^2 \right) + 2\tau \sum_{n=2}^j z_n + 6\tau \sum_{n=2}^j x_n. \end{split}$$

From the above, we arrive at

$$(4.10) (1-6\tau)x_j \le 5x_1 + x_0 + 4C_0h^2\tau \sum_{n=2}^{j} \left( |G_r^{(n)}|^2 + |G_l^{(n)}|^2 \right) + 2\tau \sum_{n=2}^{j-1} z_n + 6\tau \sum_{n=2}^{j-1} x_n.$$

The direct application of the Gronwall inequality to (4.10) produces

$$x_j \le C \left( x_1 + x_0 + \tau \sum_{n=2}^{j} \left( h^2 |G_r^{(n)}|^2 + h^2 |G_l^{(n)}|^2 + z_n \right) \right).$$

Recalling the definition of  $x_j$  and  $z_j$ , we have

$$\|\phi^{(j)}\|_h^2 \le C \left( \|\phi^{(0)}\|_h^2 + \|\phi^{(1)}\|_h^2 + \tau \sum_{n=2}^j \left( h^2 |G_r^{(n)}|^2 + h^2 |G_l^{(n)}|^2 + \|f^{(n)}\|_h^2 \right) \right).$$

(ii) For nonlocal problem with  $\delta > 0$ , applying the Cauchy inequality and the facts  $b_n \geq 0$  and  $h(\mathbf{\Phi}_{*,0}^{(n)}, \mathbf{\Phi}_{*,0}^{(n)}) \leq \|\phi^{(n)}\|_h^2 = x_n$  to the last inequality in (4.9), we derive

$$x_{j} \leq 5x_{1} + x_{0} + 2\tau \sum_{n=2}^{j} z_{n} + 2\tau \sum_{n=2}^{j} x_{n}$$

$$+ 2h\tau \sum_{n=2}^{j} \left( \|\Phi_{r,0}^{(n)}\|_{2}^{2} + \|\Phi_{l,0}^{(n)}\|_{2}^{2} + \|\mathbf{G}_{r}^{(n)}\|_{2}^{2} + \|\mathbf{G}_{l}^{(n)}\|_{2}^{2} \right)$$

$$\leq 5x_{1} + x_{0} + 2h\tau \sum_{n=2}^{j} \left( \|\mathbf{G}_{r}^{(n)}\|_{2}^{2} + \|\mathbf{G}_{l}^{(n)}\|_{2}^{2} \right) + 2\tau \sum_{n=2}^{j} z_{n} + 6\tau \sum_{n=2}^{j} x_{n}.$$

From the above, we arrive at

$$(4.11) (1 - 6\tau)x_j \le 5x_1 + x_0 + 2h\tau \sum_{n=2}^{j} \left( \|\mathbf{G}_r^{(n)}\|_2^2 + \|\mathbf{G}_l^{(n)}\|_2^2 \right) + 2\tau \sum_{n=2}^{j-1} z_n + 6\tau \sum_{n=2}^{j-1} x_n.$$

The direct application of the Gronwall inequality to (4.11) produces

$$x_j \le C \left( x_1 + x_0 + \tau \sum_{n=2}^{j} \left( h \| \mathbf{G}_r^{(n)} \|_2^2 + h \| \mathbf{G}_l^{(n)} \|_2^2 + z_n \right) \right).$$

Recalling the definitions of  $x_i$  and  $z_i$ , we have

$$\|\phi^{(j)}\|_h^2 \le C \left( \|\phi^{(0)}\|_h^2 + \|\phi^{(1)}\|_h^2 + \tau \sum_{n=2}^j \left( h \|\mathbf{G}_r^{(n)}\|_2^2 + h \|\mathbf{G}_l^{(n)}\|_2^2 + \|f^{(n)}\|_h^2 \right) \right).$$

This completes the proof.

4.2. Error estimate. From the above analysis, we first use the central difference scheme to discretize the local spatial operator and use an asymptotically compatible scheme to discretize the nonlocal spatial operator, then we apply BDF2 to approximate the temporal derivative to achieve a fully discrete infinity system. According to Taylor expansion, we obtain that the truncation error is in the order of  $\mathcal{O}(\tau^2 + h^2)$ . After that, we solve the discrete matrix (or scalar) difference equation on the exterior domain by recursive technique, and derive the exact DtD-type ABCs (2.22) and (2.24), where the coefficients (2.21) are obtained by the inverse z-transform. Finally, we reformulate the DtD-type ABCs into DtN-type ABCs, and derive the reduced problem (2.33). Now that the ABCs are exact, we have that the solution of (2.33) is the same as the solution of (2.5) confined to the computational domain.

Let  $q_*^{(n)} = (q(x_1, t_n), \dots, q(x_M, t_n))$  denote the nodal values of the exact solution of (1.2), and let  $q^{(n)} = (q_1^{(n)}, \dots, q_M^{(n)})$  be the numerical solution given by the scheme (3.15). Let  $\phi^{(n)} = q_*^{(n)} - q^{(n)}$  denote the error functions. To obtain the error estimate of the fast algorithm, we need investigate the truncated errors on  $f_k^n$  and  $G_\ell^{(n)}$  and  $G_\ell^{(n)}$  due to the stability analysis in Theorem 4.1. To the end, it is straightforward to verify that the error functions satisfy (4.1) with

$$f_k^{(n)} = \mathcal{D}_{\tau} q_k^{(n)} - \partial_t q(x_k, t_n) + \mathcal{L}_h q_k^{(n)} - \mathcal{L} q(x_k, t_n).$$

By using Taylor expansion, we have

$$||f^{(n)}||_h \le C(\tau^2 + h^2), \quad 0 \le n \le N_T.$$

The errors  $G_{\ell}^{(n)}$  and  $\mathbf{G}_{\ell}^{(n)}$  for the discrete DtN-type ABCs arise mainly from the convolution approximation. Specifically, for the local problem, we have

(4.12) 
$$hG_{\ell}^{(n)} = hA^{T}(\tilde{\mathcal{K}} - \mathcal{K}) * Q_{\ell,0}^{(n)}, \quad \ell \in \{l, r\}.$$

For the nonlocal problem with  $\delta = \mathcal{O}(1)$ , we have

(4.13) 
$$\sqrt{h}\mathbf{G}_{\ell}^{(n)} = \sqrt{h}A^{T}(\tilde{\mathcal{K}} - \mathcal{K}) * \mathbf{Q}_{\ell,0}^{(n)}, \quad \ell \in \{l, r\}.$$

By the definition (3.7), Theorem 3.1, and parameters chosen in (3.12), we have

In fact, from (4.12), (4.13), and (4.14), we have

$$(4.15) \qquad \begin{cases} h|G_{\ell}^{(n)}| \leq Ch\|A^T\|_{\infty} \|\tilde{\mathcal{K}} - \mathcal{K}\|_2 \leq C\varepsilon hN_T \|A^T\|_{\infty}, \\ \|\mathbf{G}_{\ell}^{(n)}\|_h \leq C\sqrt{h}\|A^T\|_{\infty} \|\tilde{\mathcal{K}} - \mathcal{K}\|_2 \leq C\varepsilon\sqrt{h}N_T \|A^T\|_{\infty}, \end{cases}$$

where A is given in (2.17) with the estimate

(4.16) 
$$||A^T||_{\infty} = \begin{cases} \mathcal{O}(h^{-2}) & \text{local problem,} \\ \mathcal{O}(h^{-2\nu}) & \text{nonlocal problem,} \end{cases}$$

with  $0 < \nu < 1$ . We point out that the infinity norm  $||A^T||_{\infty}$  depends on the discrete coefficients  $c_k$  for nonlocal operator in (2.8). When we consider the nonintegrable kernel  $\gamma(\alpha,\beta) = \frac{2-2\nu}{\delta^2-2\nu}\alpha^{-1-2\nu}$  with  $0 < \nu < 1$ , we have  $c_k = \mathcal{O}(h^{-2\nu})$  by using the discrete scheme in [39, page 14, Example 5].

Overall, from (4.15) and (4.16), we can take  $\varepsilon = \tau^3 h/T$  for the local problem and  $\varepsilon = \tau^3 h^{2\nu - \frac{1}{2}}/T$  for the nonlocal problem to ensure the following estimates:

$$\begin{cases} h|G_{\ell}^{(n)}| \leq C\tau^2, & \ell \in \{l,r\}, \quad 0 \leq n \leq N_T \quad \text{local problem,} \\ \|\mathbf{G}_{\ell}^{(n)}\|_h \leq C\tau^2, & \ell \in \{l,r\}, \quad 0 \leq n \leq N_T \quad \text{nonlocal problem.} \end{cases}$$

Combining the truncated error analysis above and the stability analysis in Theorem 4.1, we directly have the following convergence analysis.

THEOREM 4.2. Assume the condition (3.1) is satisfied and that the solutions of local problem (1.1) and nonlocal problem (1.2) are sufficiently smooth. For the local problem with  $\delta = 0$  and  $\varepsilon = \tau^3 h/T$ , and the nonlocal problem with  $\delta > 0$  and  $\varepsilon = \tau^3 h^{2\nu - \frac{1}{2}}/T$ , if  $\tau \leq \tau_0$  and the parameters are chosen as that in (3.12), then the following error estimate holds:

$$\max_{0 \le n \le N_T} \|\phi^{(n)}\|_h \le C(\tau^2 + h^2).$$

We remark that noting that  $\varepsilon = \tau^3 h/T$  for the local problem and  $\varepsilon = \tau^3 h^{2\nu - \frac{1}{2}}/T$  for the nonlocal problem from Theorem 4.2, the evaluation of (3.19) has the computational complexity on the order of  $\mathcal{O}(N_m N_T L^2)$  through the recurrence relations (3.16)–(3.18). Using the choice of the parameters in (3.12), we have  $N_m = \mathcal{O}(\log^2 N_T \log 1/h)$ . Thus, the computational cost for the fast algorithm is on the order of  $\mathcal{O}(L^2 N_T \log^2 N_T \log 1/h)$ , which significantly reduces the direct evaluation (2.33) with the complexity of  $\mathcal{O}(L^2 N_T^2)$  for long-time or small-time-step simulations.

We further point out that, from Theorem 4.2, we require  $\varepsilon = \tau^3 h/T$  for the local problem and  $\varepsilon = \tau^3 h^{2\nu - \frac{1}{2}}/T$  for the nonlocal problem to have the optimal convergence order. The reason is that we simply use the  $\ell_2$ -norm to present the stability analysis for the nonlocal problem in Theorem 4.1. On the other hand, for the approximation of the contour integral (3.3) by the numerical scheme (3.5), the grid step  $\tilde{\tau}$  to approximate the contour integral is the order of  $\tilde{\tau} = \mathcal{O}(-1/\log \varepsilon)$ . Thus, comparing  $\tilde{\tau} = \mathcal{O}(-1/(3\log \tau + \log h))$  for local problem, the grid step  $\tilde{\tau} = \mathcal{O}(-1/(3\log \tau + (2\nu - 1/2)\log h))$  for nonlocal problem. It leads to a refined grid

step  $\tilde{\tau}$  with the increment of  $\mathcal{O}(-1/\log h)$  to calculate the convolution coefficients  $\tilde{K}_j$   $(j=1,\ldots,N_T)$  to improve their accuracy. This implies that the extra computational complexity for the evaluation of  $\tilde{K}_j$  for each j in (3.9) with a refined  $\tilde{\tau}$  is in the order of  $\mathcal{O}(\log N_T \log 1/h)$ . When combining the fast algorithm (3.16)–(3.18) to evolve the model equation, the total extra computational complexity is in the order of  $\mathcal{O}(L^2N_T\log^2 N_T \log 1/h)$ .

5. Numerical examples. We now embark on numerical examples to demonstrate the effectiveness of our approach in various aspects: (i) the spatial and time convergence of numerical scheme (3.15) for the local problem; (ii) the spatial and time convergence of the numerical scheme (3.15) to the nonlocal problem (1.2) by fixing  $\delta$  and refining  $h \leq \delta$  and  $\tau$ ; (iii) the asymptotic compatibility of the numerical scheme by refining  $\delta$  and h simultaneously; (iv) the computational efficiency of the fast scheme (3.15) compared with the direct scheme (2.33).

In all simulations below, the Gaussian initial value is used as

$$q(x,0) = \sqrt{\frac{5}{\pi}} \exp(-5(x-0.2)^2),$$

and three typical kernels are respectively taken as

- 1. the constant integral kernels  $\gamma(\alpha, \beta) = 3\delta^{-3}$  for  $\alpha \in [-\delta, \delta]$ ;
- 2. the nonintegral kernel  $\gamma(\alpha, \beta) = 2\alpha^{-1}\delta^{-2}$  for  $\alpha \in (0, \delta]$ ;
- 3. the inhomogeneous kernel

(5.1) 
$$\gamma(\alpha, \beta) = \frac{40\sqrt{10}\sigma}{\sqrt{\pi}\xi^3} \exp\left(-\frac{10\alpha^2}{\xi^2}\right)$$

with  $\xi = \delta (1 + \operatorname{erfc}(\beta)/4)$  and  $\sigma = 1 + \exp(-3\beta^2)$ .

Example 1 (local convergence):  $\ell^2$ -errors and spatial convergence orders.

h	$2^{-2}$	$2^{-3}$	$2^{-4}$	$2^{-5}$	$2^{-6}$
$\ell^2$ -errors order	$5.49 \times 10^{-4}$	$1.35 \times 10^{-4} \\ 2.02$	$3.36 \times 10^{-5}$ $2.01$	$8.38 \times 10^{-6}$ $2.00$	$2.09 \times 10^{-6} \\ 2.00$

Example 1. We first consider the local problem

$$q_t = q_{xx}$$

with the exact solution given by

$$q(x,t) = \frac{1}{\sqrt{4\pi(t+0.05)}} \exp\left(-\frac{(x-0.2)^2}{4(t+0.05)}\right).$$

For all simulations, we take the computational domain  $\Omega = [-3, 3]$  and the final time T = 2. We verify the spatial convergence order by refining the spatial size h and setting the time step  $\tau = 5 \times 10^{-4}$ , and we test the time convergence order by refining the time step  $\tau$  and setting the spatial step  $h = 2^{-8}$ . Table 1 shows second-order spatial convergences and Table 2 shows second-order time convergence.

Example 2. We then consider the constant integral kernel  $\gamma(\alpha, \beta) = 3\delta^{-3}$  for  $\alpha \in [-\delta, \delta]$ , which only depends on the first parameter  $\alpha$ . In this situation, the

Table 2 Example 1 (local convergence):  $\ell^2$ -errors and time convergence orders.

au	$2^{-2}$	$2^{-3}$	$2^{-4}$	$2^{-5}$	2-6
$\ell^2$ -errors order	$6.81 \times 10^{-3}$	$1.44 \times 10^{-3} \\ 2.24$	$3.38 \times 10^{-4}$ $2.09$	$8.16 \times 10^{-5} \\ 2.05$	$2.00 \times 10^{-5} \\ 2.03$

pseudo-spectral method is used to calculate the reference solution by solving the nonlocal problem over a larger domain with sufficiently fine mesh sizes.

By taking  $\delta=0.5,1,2$ , respectively, Table 3 shows the  $\ell^2$ -errors and spatial convergence orders of numerical solutions of discrete scheme (3.15) by refining mesh sizes h with the same parameters as those in Example 1. Table 4 shows the  $\ell^2$ -errors and time convergence orders of numerical solutions of discrete scheme (3.15) by refining mesh sizes  $\tau$  with the same parameters as those in Example 1. Table 5 shows asymptotic compatibility for our scheme. One can see that scheme (3.15) has second-order convergence rate.

Table 3 Example 2 (nonlocal convergence):  $\ell^2$ -errors and spatial convergence orders.

$h$ $\delta$	$\delta = 2$ Orde	er	$\delta = 1$ Ord	der	$\delta = 0.5$ O	rder
$2^{-2}$	$6.86 \times 10^{-4}$		$3.03 \times 10^{-4}$		$2.68 \times 10^{-4}$	
$2^{-3}$	$1.69 \times 10^{-4}$ 2	2.02	$7.55 \times 10^{-5}$	2.00	$6.86 \times 10^{-5}$	1.96
$2^{-4}$	$4.20 \times 10^{-5}$ 2		$1.88 \times 10^{-5}$	2.01	$1.72 \times 10^{-5}$	
$2^{-5}$	$1.05 \times 10^{-5}$ 2			2.01	$4.30 \times 10^{-6}$	
$2^{-6}$	$2.60 \times 10^{-6}$ 2	2.01	$1.15 \times 10^{-6}$	2.02	$1.07 \times 10^{-6}$	2.00

Table 4 Example 2 (nonlocal convergence):  $\ell^2$ -errors and time convergence orders.

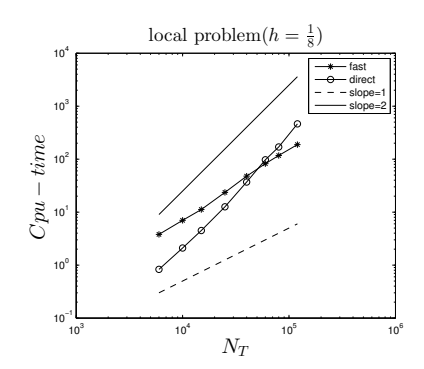
$\tau$ $\delta$	$\delta = 2$ Order	$\delta = 1$ Order	$\delta = 0.5$ Order	
$2^{-2}$ $2^{-3}$	$9.15 \times 10^{-3}$ $1.95 \times 10^{-3}$ 2.23		$\begin{array}{cccc} 6.98 \times 10^{-3} & \\ 1.47 \times 10^{-3} & 2.25 \end{array}$	
$2^{-4}$	$4.56 \times 10^{-4}$ 2.10	$3.99 \times 10^{-4}$ 1.97	$3.66 \times 10^{-4}$ 2.00	
$2^{-5}$ $2^{-6}$	$1.07 \times 10^{-4}$ $2.09$ $2.45 \times 10^{-5}$ $2.13$		$\begin{array}{ccc} 8.04 \times 10^{-5} & 2.19 \\ 1.95 \times 10^{-5} & 2.05 \end{array}$	

 ${\it TABLE~5} \\ {\it Example~2~(local~limit):~} \ell^2\text{-errors~and~spatial~convergence~orders}.$ 

b	$\delta = h$ Order		$\delta = 2h$ Order		$\delta = 3h$ Order	
$2^{-2}$	$5.49 \times 10^{-4}$		$1.60 \times 10^{-3}$		$3.34 \times 10^{-3}$	
$2^{-3}$	$1.35 \times 10^{-4}$		$3.90 \times 10^{-4}$	2.03	$8.03 \times 10^{-4}$	
$2^{-4}$	$3.36 \times 10^{-5}$		$9.67 \times 10^{-5}$		$1.98 \times 10^{-4}$	
$2^{-5}$	$8.36 \times 10^{-6}$	-	$2.41 \times 10^{-5}$		$4.93 \times 10^{-5}$	
$2^{-6}$	$2.07 \times 10^{-6}$	2.01	$5.99 \times 10^{-6}$	2.01	$1.23 \times 10^{-5}$	2.00

We now check the computational costs by comparing the fast scheme (3.15) with the direct scheme (2.33) for both the local problem and the nonlocal problem. The CPU time is calculated by taking the total temporal step  $N_T = [0.6, 1, 1.5, 2.5, 4, 6, 8, 12]$ 

 $\times 10^4$  with a fixed spatial mesh size h=1/8, and using the parameters given in (3.12). Figure 2 clearly shows the  $O(N_T^2)$  complexity for the direct algorithm (2.33), and the essential  $O(N_T \log^2 N_T)$  complexity of the fast method (3.15) for both local and non-local problems. That is, the fast scheme significantly reduces the computational cost as  $N_T$  is larger and larger.



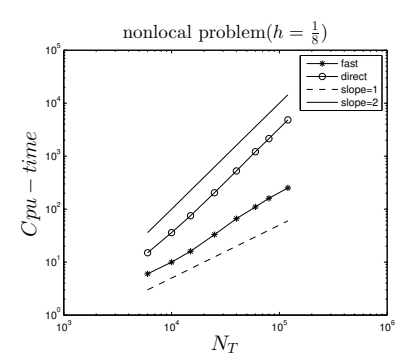


Fig. 2. The CPU-time for different total time steps  $N_T$  with h = 1/8. Left: local problem. Right: nonlocal problem.

Example 3. We use this example to consider the nonintegral kernel  $\gamma(\alpha,\beta)=2\alpha^{-1}\delta^{-2}$  for  $\alpha\in[0,\delta]$ , and again use the pseudo-spectral method to achieve the reference solution. Table 6 shows second-order spatial convergences by refining the spatial size h for any given  $\delta$  by using fast scheme (3.15) with the same parameters as those used in Example 1.

Table 6 Example 3 (nonlocal convergence):  $\ell^2$ -errors and spatial convergence orders.

b	$\delta = 2$ order	$\delta = 1$ Order	$\delta = 0.5$ Order	
$ \begin{array}{r} 2^{-2} \\ 2^{-3} \\ 2^{-4} \\ 2^{-5} \\ 2^{-6} \end{array} $	$\begin{array}{cccccc} 4.75\times 10^{-4} &\\ 1.17\times 10^{-4} & 2.02\\ 2.92\times 10^{-5} & 2.00\\ 7.29\times 10^{-6} & 2.00\\ 1.83\times 10^{-6} & 1.99 \end{array}$	$3.00 \times 10^{-4}$ $7.42 \times 10^{-5}$ 2.02 $1.85 \times 10^{-5}$ 2.01 $4.61 \times 10^{-6}$ 2.00 $1.16 \times 10^{-6}$ 1.99	$\begin{array}{cccccccccccccccccccccccccccccccccccc$	

Example 4. We use this example to consider the inhomogeneous kernel given in (5.1). In this situation, noting that the diffusion coefficient is inhomogeneous, the pseudo-spectral method is not available to compute the reference solution. Alternatively, we use the fast scheme (3.15) to achieve the reference solutions with sufficiently fine mesh size. Again, using the fast scheme with the same parameters as that in Example 1, Table 7 shows second-order spatial convergences by refining the spatial size h for any given  $\delta$ .

6. Conclusion. A stable, fast, and second-order approximation scheme is developed for numerically solving both local and nonlocal diffusion equations on the unbounded spatial domain. To present the error estimate of the proposed scheme, the key step is to construct the DtN-type ABCs for the fully discrete system whenever it arises from the local or nonlocal problems. After that, we use the technique developed in [22, 23, 27, 28] to design a fast algorithm of the ABCs. Finally, we established the stability and error analysis for our proposed scheme with fast evaluations of ABCs

Table 7

Example 4 (nonlocal convergence):  $\ell^2$ -errors and spatial convergence orders.

$\delta$	$\delta = 0.5$ Order	$\delta = 0.4$ Order	$\delta = 0.3$ Order
$2^{-2}$	$2.27 \times 10^{-4}$	$2.83 \times 10^{-4}$	$3.26 \times 10^{-4}$
$2^{-3}$	$6.83 \times 10^{-5}$ 2.02	$6.79 \times 10^{-5}$ 2.06	$6.76 \times 10^{-5}$ 2.27
$2^{-4}$	$1.69 \times 10^{-5}$ 2.01	$1.68 \times 10^{-5}$ 2.02	$1.66 \times 10^{-5}$ 2.02
$2^{-5}$	$4.15 \times 10^{-6}$ 2.03	$4.11 \times 10^{-6}$ 2.03	$4.06 \times 10^{-6}$ 2.04
$2^{-6}$	$9.81 \times 10^{-7}$ 2.08	$9.69 \times 10^{-7}$ 2.09	$9.52 \times 10^{-7}$ 2.09

based on some sectorial properties of the associated operator  $\hat{\mathcal{K}}$ . While the latter remains open, in all simulations, no numerical instability and second-order convergence had been observed. As far as we know, this is the first work on establishing a common framework to design DtN-type ABCs for both local and nonlocal problems with fast algorithms to evaluate the ABCs.

In this paper, we only consider the local problem and the nonlocal problem with  $\delta = \mathcal{O}(1)$ . As the horizon  $\delta \to 0$ , it is known that nonlocal operators will converge to local operators; see (1.5). It is natural to ask if the discrete approximation (3.15) converges to the local problem as both  $\delta$  and  $h \to 0$ , that is, if the approximation is truly asymptotically compatible in the sense of [31, 32, 33] in light of the additional approximations. The corresponding stability analysis in Theorem 4.1 remains open. This is beyond the scope of this paper and will be left to future studies.

## Appendix A.

The proof of Lemma 3.1. Based on the condition (3.1) and using the similar techniques in [23], it is straightforward to verify

$$\|\mu\tau\hat{\mathcal{K}}(\gamma(\theta+i\beta))\cos(\alpha+i(\theta+i\beta))\|_{2} \leq M\tau\sqrt{\frac{1+\sin(\alpha+d)}{1-\sin(\alpha-d)}} := \frac{M_{0}}{2} \quad \forall \theta \in \mathbb{R},$$

$$\left|\frac{1}{2-\sqrt{1+2\tau\gamma(\theta+i\beta)}}\right| \leq \frac{1}{\sqrt{(1+\mu\tau\cosh\theta)(1-\mu\tau)}} \quad \forall \theta \geq \ln\left(\frac{56}{\mu\tau}+2\right),$$

$$\left|\frac{1}{\sqrt{1+2\tau\gamma(\theta+i\beta)}}\right| \leq 2 \quad \forall \theta \in \mathbb{R}.$$

Recalling the definition of  $G_k(\theta + i\beta)$  in (3.4) and noting the estimates above, we have the desired result that

$$||G_k(\theta + i\beta)||_2 \le \frac{M_0}{\sqrt{(1 + \mu\tau \cosh \theta)^{k+1}(1 - \mu\tau)^{k+1}}}.$$

This completes the proof.

The proof of Lemma 3.3. Using the results in Lemmas 3.1 and 3.2, and noting the facts that

$$(1 - y/k)^{-(k+1)} \le 2 \exp(2y)$$
 for  $0 \le y \le k/2$ ,  
 $\phi(y) \le 8$  for  $y \ge 0.01$ ,

we have

$$N(G_{k}, D_{d}) := 2 \left( \int_{N\tilde{\tau}}^{+\infty} + \int_{0}^{N\tilde{\tau}} \right) (\|G_{k}(\theta + id)\|_{2} + \|G_{k}(\theta - id)\|_{2}) d\theta$$

$$\leq 4 \int_{N\tilde{\tau}}^{+\infty} \frac{M_{0}}{(1 - \mu t/k)^{\frac{k+1}{2}}} \left( 1 + \frac{\mu t}{k} \cosh \theta \right)^{-\frac{k+1}{2}} d\theta$$

$$+ 2 \int_{0}^{N\tilde{\tau}} (\|G_{k}(\theta + id)\|_{2} + \|G_{k}(\theta - id)\|_{2}) d\theta$$

$$\leq 4\sqrt{2}M_{0} \exp(\mu t) \left( 8 \exp\left( -\frac{\mu t \cosh(N\tilde{\tau})}{4} \right) + \left( 1 + \frac{\mu t}{k} \cosh(N\tilde{\tau}) \right)^{-\frac{k-1}{2}} \right)$$

$$+ 8M_{0}N\tilde{\tau} \exp(2\mu t)$$

$$\leq 9M_{0}N\tilde{\tau} \exp(2\mu t).$$

The proof of Theorem 3.1.

*Proof.* Denote

$$E_{\tilde{\tau},\infty}(G_k) = \int_{-\infty}^{+\infty} G_k(\theta) d\theta - \tilde{\tau} \sum_{n=-\infty}^{\infty} G_k(n\tilde{\tau}).$$

For any fixed  $N \geq 1$ , it is easy to verify that

$$||E_{\tilde{\tau},N}(G_k)||_2 \le ||E_{\tilde{\tau},\infty}(G_k)||_2 + \tilde{\tau} \sum_{|n|>N+1} ||G_k(n\tilde{\tau})||_2.$$

By Theorem 4.1 in [27] (see also [28]), we have

$$||E_{\tilde{\tau},\infty}(G_k)||_2 \le \frac{N(G_k, D_d)}{e^{2\pi d/\tilde{\tau}} - 1} \le 10M_0N\tilde{\tau}\exp\left(2\mu t - \frac{2\pi d}{\tilde{\tau}}\right).$$

Moreover, we have

$$\tilde{\tau} \sum_{|n| \ge N+1} \|G_k(n\tilde{\tau})\|_2 \le 2 \sum_{n=N+1}^{+\infty} \frac{M_0}{(1 - \mu t/k)^{\frac{k+1}{2}}} \left(1 + \frac{\mu t}{k} \cosh(n\tilde{\tau})\right)^{-\frac{k+1}{2}}$$

$$\le \frac{2M_0}{(1 - \mu t/k)^{\frac{k+1}{2}}} \int_{N\tilde{\tau}}^{+\infty} \left(1 + \frac{\mu t}{k} \cosh\theta\right)^{-\frac{k+1}{2}} d\theta$$

$$\le 2\sqrt{2}M_0 \exp(\mu t) \left(8 \exp\left(-\frac{\mu t \cosh(N\tilde{\tau})}{4}\right) + \left(1 + \frac{\mu t}{k} \cosh(N\tilde{\tau})\right)^{-\frac{k-1}{2}}\right).$$

Overall, we arrive at

$$||E_{\tilde{\tau},N}(G_k)||_2 \leq 10M_0N\tilde{\tau}\exp\left(2\mu t - \frac{2\pi d}{\tilde{\tau}}\right) + 16\sqrt{2}M_0\exp\left(\mu t - \frac{\mu t\cosh(N\tilde{\tau})}{4}\right) + 2\sqrt{2}M_0\exp(\mu t)\left(1 + \frac{\mu t}{k}\cosh(N\tilde{\tau})\right)^{-\frac{k-1}{2}}.$$

## REFERENCES

- D. A. Anderson, J. C. Tannehill, and R. H. Pletcher, Computational Fluid Mechanics and Heat Transfer, 3rd ed., CRC Press, Boca Raton, FL, 2013.
- B. Alpert, L. Greengard, and T. Hagstrom, Rapid evaluation of nonreflecting boundary kernels for time-domain wave propagation, SIAM J. Numer. Anal., 37 (2000), pp. 1138– 1164, https://doi.org/10.1137/S0036142998336916.
- [3] X. Antoine and C. Besse, Unconditionally stable discretization schemes of non-reflecting boundary conditions for the one-dimensional Schrödinger equation, J. Comput. Phys., 188 (2003), pp. 157–175.
- [4] A. Arnold, M. Ehrhardt, and I. Sofronov, Discrete transparent boundary conditions for the Schrödinger equation: Fast calculation, approximation, and stability, Commun. Math. Sci., 1 (2003), pp. 501–556.
- [5] O. BOKANOWSKI, A. PICARELLI, AND C. REISINGER, Stability and Convergence of Second Order Backward Differentiation Schemes for Parabolic Hamilton-Jacobi-Bellman Equations, preprint, https://arxiv.org/abs/1802.07146, 2018.
- [6] X. CAO AND H. LIU, Determining a Fractional Helmholtz System with Unknown Source and Medium Parameter, preprint, https://arxiv.org/abs/1803.09538, 2018, Commun. Math. Sci., in press.
- [7] X. CAO, Y. LIN, AND H. LIU, Simultaneously recovering potentials and embedded obstacles for anisotropic fractional Schrödinger operators, Inverse Probl. Imaging, 13 (2019), pp. 197–210.
- [8] Q. Du, Nonlocal Modeling, Analysis and Computation, CBMS-NSF Regional Conf. Ser. in Appl. Math. 94, SIAM, Philadelphia, 2019, https://doi.org/10.1137/1.9781611975628.
- [9] Q. Du, M. Gunzburger, R. B. Lehoucq, and K. Zhou, Analysis and approximation of nonlocal diffusion problems with volume constraints, SIAM Rev., 54 (2012), pp. 667–696, https://doi.org/10.1137/110833294.
- [10] Q. Du, H. Han, J. Zhang, and C. Zheng, Numerical solution of a two-dimensional nonlocal wave equation on unbounded domains, SIAM J. Sci. Comput., 40 (2018), pp. 1430–1445, https://doi.org/10.1137/16M1102896.
- [11] Q. Du, J. Zhang, and C. Zheng, Nonlocal wave propagation in unbounded multiscale media, Commun. Comput. Phys., 24 (2018), pp. 1049-1072.
- [12] Q. Du, J. Zhang, and C. Zheng, On uniform second order nonlocal relaxations to linear two-point boundary value problems, Commun. Math. Sci., 17 (2019), pp. 1737–1755.
- [13] D. GIVOLI, High-order local non-reflecting boundary conditions: A review, Wave Motion, 39 (2004), pp. 319–326.
- [14] L. GREENGARD AND P. LIN, On the Numerical Solution of the Heat Equation in Unbounded Domains (Part I), Tech. Note 98-002, Courant Mathematics and Computing Laboratory, New York University, New York, 1998.
- [15] T. HAGSTROM, New Results on Absorbing Layers and Radiation Boundary Conditions, in Topics in Computational Wave Propagation, M. Ainsworth et al., eds., Springer-Verlag, New York, 2003, pp. 1–42.
- [16] H. HAN AND Z. HUANG, A class of artificial boundary conditions for heat equation in unbounded domains, Comput. Math. Appl., 43 (2002), pp. 889–900.
- [17] H. HAN AND D. YIN, Numerical solutions of parabolic problems on unbounded 3-D spatial domain, J. Comput. Math., 23 (2005), pp. 449–462.
- [18] H. HAN AND X. WU, Artificial Boundary Method, Spring-Verlag and Tsinghua University Press, Berlin, Heidelberg, and Beijing, 2013.
- [19] S. D. JIANG AND L. GREENGARD, Fast evaluation of nonreflecting boundary conditions for the Schrödinger equation in one dimension, Comput. Math. Appl., 47 (2004), pp. 955–966.
- [20] B. LI, J. ZHANG, AND C. ZHENG, An efficient second-order finite difference method for the onedimensional Schrödinger equation with absorbing boundary conditions, SIAM J. Numer. Anal., 56 (2018), pp. 766–791, https://doi.org/10.1137/17M1122347.
- [21] B. Li, J. Zhang, and C. Zheng, Stability and error analysis for a second-order fast approximation of the 1d Schrödinger equation under absorbing boundary conditions, SIAM J. Sci. Comput., 40 (2018), pp. A4083–A4104, https://doi.org/10.1137/17M1162111.
- [22] M. LÓPEZ-FERNANDEZ, C. LUBICH, C. PALENCIA, AND A. SCHÄDLE, Fast Runge-Kutta approximation of inhomogeneous parabolic equations, Numer. Math., 102 (2005), pp. 277–291.
- [23] M. LÓPEZ-FERŃANDEZ AND C. PALENCIA, On the numerical inversion of the Laplace transform of certain holomorphic mappings, Appl. Numer. Math., 51 (2004), pp. 289–303.
- 24] C. Lubich and A. Schädle, Fast convolution for nonreflecting boundary conditions, SIAM J. Sci. Comput., 24 (2002), pp. 161–182, https://doi.org/10.1137/S1064827501388741.

- [25] G. Pang, Y. Yang, and S. Tang, Exact boundary condition for semi-discretized Schrödinger equation and heat equation in a rectangular domain, J. Sci. Comput., 72 (2017), pp. 1–13.
- [26] S. S. RAVINDRAN, An extrapolated second order backward difference time-stepping scheme for the magnetohydrodynamics system, Numer. Funct. Anal. Optim., 37 (2016), pp. 990–1020.
- [27] F. STENGER, Approximations via Whittaker's cardinal function, J. Approx. Theory, 17 (1976), pp. 222–240.
- [28] F. STENGER, Numerical methods based on Whittaker's cardinal, or sinc functions, SIAM Rev., 23 (1981), pp. 165–224, https://doi.org/10.1137/1023037.
- [29] Z. Z. Sun and X. Wu, The stability and convergence of a difference scheme for the Schrödinger equation on an infinite domain by using artificial boundary conditions, J. Comput. Phys., 214 (2006), pp. 209–223.
- [30] Y. TAO, X. TIAN, AND Q. Du, Nonlocal diffusion and peridynamic models with Neumann type constraints and their numerical approximations, Appl. Math. Comput., 305 (2017), pp. 282–298.
- [31] X. Tian and Q. Du, Analysis and comparison of different approximations to nonlocal diffusion and linear peridynamic equations, SIAM J. Numer. Anal., 51 (2013), pp. 3458–3482, https: //doi.org/10.1137/13091631X.
- [32] X. TIAN AND Q. Du, Asymptotically compatible schemes and applications to robust discretization of nonlocal models, SIAM J. Numer. Anal., 52 (2014), pp. 1641–1665, https: //doi.org/10.1137/130942644.
- [33] X. Tian and Q. Du, Asymptotically compatible schemes for robust discretization of parametrized problems with applications to nonlocal models, SIAM Rev., 62 (2020), pp. 199–227, https://doi.org/10.1137/19M1296720.
- [34] S. V. TSYNKOV, Numerical solution of problems on unbounded domains: A review, Appl. Numer. Math., 27 (1998), pp. 465–532.
- [35] X. N. Wu And Z. Z. Sun, Convergence of difference scheme for heat equation in unbounded domains using artificial boundary conditions, Appl. Numer. Math., 50 (2004), pp. 261–277.
- [36] X. Wu And J. Zhang, High-order local absorbing boundary conditions for heat equation in unbounded domains, J. Comput. Math., 29 (2011), pp. 74-90.
- [37] W. ZHANG, J. YANG, J. ZHANG, AND Q. Du, Absorbing boundary conditions for nonlocal heat equations on unbounded domain, Commun. Comput. Phys., 21 (2017), pp. 16–39.
- [38] C. Zheng, Approximation, stability and fast evaluation of exact artificial boundary condition for one-dimensional heat equation, J. Comput. Math., 25 (2007), pp. 730–745.
- [39] C. ZHENG, J. HU, Q. DU, AND J. ZHANG, Numerical solution of the nonlocal diffusion equation on the real line, SIAM J. Sci. Comput., 39 (2017), pp. 1951–1968, https://doi.org/10.1137/ 16M1090107.
- [40] K. Zhou and Q. Du, Mathematical and numerical analysis of linear peridynamic models with nonlocal boundary conditions, SIAM J. Numer. Anal., 48 (2010), pp. 1759–1780, https://doi.org/10.1137/090781267.